be narrower and this is observed. ($C_2$ could experience coupling to $H_7$, but, in view of the bending away of the uncomplexed double bond, the coupling is expected to be reduced in comparison with coupling in a planar fragment). Distinction between $C_2$ and $C_4$ was made on the basis of higher temperature spectra. The D $\rightleftharpoons$ D′ (degenerate) process exchanges $C_3$ with $C_2$ and spectra at −50 and −35 °C show that the 105.6-ppm signal ($C_3$) averages with the 104.7-ppm signal and not the remaining 107.5-ppm signal. Hence $C_2$ is at 104.7 ppm. (The averaged signal emerges quite quickly as the chemical shift separation is only ~1 ppm.) (b) H. Gunther, H. Seel, and M. E. Gunther, *Org. Magn. Reson.*, 11, 97 (1978).

# Hexakis(pyridine)ruthenium(II) Tetrafluoroborate. Molecular Structure and Spectroscopic Properties

**Joseph L. Templeton**

*Contribution from the W. R. Kenan, Jr. Laboratory, Department of Chemistry, University of North Carolina, Chapel Hill, North Carolina 27514.*
*Received January 15, 1979*

**Abstract:** Hexakis(pyridine)ruthenium(II) tetrafluoroborate has been prepared by extended reflux of a methanol solution of $[RuHS_3(PPh_3)_2][BF_4]$ (S = $CH_3OH$ or $H_2O$) and pyridine. Spectroscopic and electrochemical characterizations of this complex are reported. The observed $^1H$ and $^{13}C$ chemical shift values are discussed in terms of previous reports concerning NMR properties of complexed pyridine. A comparison of ruthenium-nitrogen force constants for pyridine and ammine ligands is based upon far-infrared vibrational data. Rationalization of the larger force constant evident in the case of pyridine is presented in terms of both $\sigma$ and $\pi$ interactions in the case of this unsaturated heterocyclic ligand. Assignment of a metal-to-ligand charge transfer band at 341 nm, in conjunction with electrochemical reduction potentials, provides data for a general qualitative molecular orbital scheme for a series of $[Ru(py)_n(NH_3)_{6-n}]^{2+}$ complexes ($n$ = 6, 2, 1, 0). The electrochemistry of $[Ru(py)_6]^{2+}$ is virtually indistinguishable from that of the $[Ru(bpy)_3]^{2+}$ ion. Crystals of $[Ru(py)_6][BF_4]_2$ were found to be orthorhombic, space group $Pna2_1$, with a unit cell of dimensions $a$ = 16.933 (27), $b$ = 10.431 (7), and $c$ = 18.197 (14) Å. The observed density is 1.54(2) g cm$^{-3}$ while a density of 1.536 g cm$^{-3}$ is calculated for $Z$ = 4. The structure was refined to $R$ = 0.063 and $R_w$ = 0.075 using 2142 reflections with $I \geq 3\sigma(I)$. The $Ru(py)_6^{2+}$ cation exhibits Ru-N bond lengths in the range from 2.10 (1) to 2.14 (1) Å with an average length of 2.12 Å for the six metal-ligand bonds. The rotational orientation of the six planar ligands is such that the isolated cation belongs to the $C_1$ point group, i.e., there is clearly no symmetry operation present other than the identity itself.

## Introduction

An extensive chemistry of ruthenium(II) complexes containing nitrogen donor ligands has been realized during the past decade.[1] The range of chemical properties accessible to such complexes is evident in the diverse properties of the two cationic derivatives $Ru(NH_3)_6^{2+}$ and $Ru(bpy)_3^{2+}$.

Hexaammineruthenium(II) is a classical octahedral coordination complex[2] containing six $\sigma$-only ammine ligands. One exceptional feature of this unit is the variety of reactions which form $Ru(NH_3)_5L^{2+}$ complexes[3] (where L is a $\pi$-acceptor ligand such as $N_2$, CO, RCN, etc.). This reactivity pattern implicates the $Ru(NH_3)_5^{2+}$ $(d\pi)^6$ fragment as a unit capable of extensive $\pi$ donation to acceptor ligands. Such a conclusion is consistent with expectations for a low-spin $d^6$ system which has the optimal number of d electrons for bonding interactions with empty ligand $\pi$ orbitals. Furthermore, the $Ru(NH_3)_5^{2+}$ moiety has no pathway available for the transfer of electron density from the metal to the five ammine ligands which are devoid of empty $\pi$-type orbitals, leaving only L as a $d\pi$ electron sink. Since effective electronegativity increases with an increase in oxidation state of the metal, the relatively low 2+ oxidation state of ruthenium (as compared to other common $d^6$ ions such as $Co^{3+}$ and $Rh^{3+}$) enhances covalent $\pi$ interactions with appropriate ligand orbitals where the metal furnishes the electron density. Thus the isolation of such noteworthy species as $Ru(NH_3)_5(N_2)^{2+}$ [4] can be rationalized in retrospect.

The tris(bipyridyl)ruthenium(II,III) couple is another octahedral ruthenium system which has attracted widespread attention owing to the unique redox and photochemical properties it displays.[5] The photoredox chemistry of this complex has been the subject of extensive research efforts directed toward the conversion of light into chemical and electrical energy.[6] The lifetime of the photochemical excited state is adequate to allow bimolecular electron transfer processes to occur which utilize the high-energy transient species as a reactant.[7]

Although reports of $M(py)_6^{n+}$ cations abound in the literature,[8] in only a few cases have crystalline solids been structurally characterized in which six pyridines remain bound to one metal ion. One study which confirmed the existence of $M(py)_6^{n+}$ in the solid state was reported for the Fe(II) cation.[9] The high-spin $d^6$ iron dication in the $[Fe(py)_6][Fe_4(CO)_{13}]$ structure conforms to $T_h$ molecular symmetry as appropriate to minimize steric repulsions among the six ligands. Doedens and Dahl concluded that in the absence of distortional forces (such as hydrogen bonding or Jahn-Teller degeneracies) a transition metal bound to six identical $C_{2v}$ ligands would presumably exist in the $T_h$ molecular form.

In view of the current interest in the chemistry of octahedral ruthenium(II,III) complexes with nitrogen donor ligands we have synthesized $[Ru(py)_6][BF_4]_2$ and now report the molecular structure as determined by X-ray crystallographic techniques as well as other relevant spectroscopic data.

Although similar values of $10Dq$ characterize py and $NH_3$ as evidenced by their approximate equivalence in the spectrochemical series,[10] the metal-ligand interactions which produce these roughly equivalent d-orbital splittings are quite different for the two nitrogenous nucleophiles. The presence of vacant pyridine $\pi^*$ molecular orbitals provides a potential pathway for $\pi$ back-bonding from ruthenium(II) to the ligands in the hexakis(pyridine)ruthenium(II) complex. Thus, in spite of the similar distribution of six monodentate nitrogen donor

0002-7863/79/1501-4906$01.00/0 

ligands about the central metal in both $Ru(NH_3)_6^{2+}$ and $Ru(py)_6^{2+}$, it was anticipated that the comparative chemistry of these two ruthenium(II) complexes would be marked by contrasts. On the other hand, $Ru(py)_6^{2+}$ might be expected to resemble $Ru(bpy)_3^{2+}$ in several important properties. Data relevant to these comparisons are reported herein for the hexakis(pyridine)ruthenium(II) cation present in $[Ru(py)_6][BF_4]_2$.

## Experimental Section

**Materials and Synthesis.** All manipulations were performed under an oxygen-free nitrogen atmosphere and solvents were degassed by purging with nitrogen gas for approximately 15 min prior to use. Schlenck techniques were employed for manipulating solids and solutions, and transfers were made by conventional syringe and serum cap techniques. Diaquahydridomethanolbis(triphenylphosphine)-ruthenium, $[RuH(H_2O)_2(MeOH)(PPh_3)_2](BF_4)$, was prepared as described by Young and Wilkinson.[11] Ruthenium trichloride hydrate from Johnson, Matthey was used as received to prepare $RuCl_2(PPh_3)_3$,[12] which was converted to $RuH(O_2CMe)(PPh_3)_3$[13] prior to preparing the $[RuH(H_2O)_2(MeOH)(PPh_3)_2](BF_4)$ starting material. Solid $[RuH(H_2O)_2(MeOH)(PPh_3)_2](BF_4)$ (420 mg, 0.54 mmol) was refluxed in a methanol (35 mL) and pyridine (5 mL) solvent mixture under nitrogen for 24 h. The yellow solid slowly dissolved as the reaction proceeded. The orange solution was filtered while hot and allowed to cool slowly to obtain the yellow, microcrystalline complex which precipitated. The solid was rinsed with degassed methanol and ether and dried in vacuo (140 mg, 35% based on Ru). Addition of methanol to the mother liquor induced formation of single crystals suitable for X-ray analysis.

Anal. Calcd for $[Ru(NC_5H_5)_6](BF_4)_2$, $C_{30}H_{30}N_6B_2F_8Ru$: C, 48.09; N, 11.22; H, 4.04. Found: C, 47.92; N, 11.01; H, 3.90.

**Physical Measurements.** Infrared spectra were obtained as Nujol mulls on CsI plates or in compressed KBr disks with a Beckman 4250 infrared spectrophotometer. A Cary 14 spectrometer was used to record electronic spectra and a Varian XL-100 FT NMR was employed to obtain both $^1H$ and $^{13}C$ NMR spectra. Conductivities were measured with a Mullard conductivity bridge Type E7566/3 using standard procedures[14] and nitromethane as solvent. Electrochemical measurements were made vs. the saturated sodium chloride calomel electrode (SCE) at 25 ± 2 °C, and are uncorrected for junction potentials. Potentials reported are reduction potentials vs. SCE. Potential control for electrochemical experiments was obtained with a Princeton Applied Research Model 173 potentiostat/galvanostat. The waveform generator for voltammetric experiments was a Princeton Applied Research Model 175 universal programmer. Voltammograms were recorded on a Hewlett-Packard Model 7004B X-Y recorder. The value of $n$, where $n$ is the total number of equivalents of electrons transferred in exhaustive electrolysis at constant potential, was calculated after measuring the total area under the current vs. time curve for complete reaction. The reaction was judged to be complete when the current had fallen below 1% of the initial value. Voltammetric measurements were carried out at platinum electrodes in solutions deaerated with a stream of dry, prepurified nitrogen. Microanalyses were performed by the Butterworth Microanalytical Consultancy, Teddington, United Kingdom.

**Collection and Reduction of X-ray Data.** Preliminary Weissenberg and precession photography indicated that $[Ru(py)_6](BF_4)_2$ crystals belonged to the orthorhombic system. The possible space groups were $Pna2_1$ or $Pnma$ as evidenced by the absence of $Okl$ reflections with $k + l = 2n + 1$ and $h0l$ reflections with $h = 2n + 1$. The noncentrosymmetric space group $Pna2_1$ was chosen, and successful refinement of the structure demonstrated that this choice was correct. A crystal of approximate dimensions 0.20 × 0.40 × 0.45 mm was chosen for diffractometer data collection. Observations were made at ambient temperature using Mo $K\alpha_1$ radiation with an assumed wavelength of 0.7093 Å. The cell constants, obtained by least-squares methods, are $a$ = 16.933 (27), $b$ = 10.431 (7), and $c$ = 18.197 (14) Å. A calculated density of 1.536 g cm$^{-3}$ assuming four molecules per unit cell compares with an observed flotation density of 1.54 (2) g cm$^{-3}$ obtained in a mixture of chloroform and carbon tetrachloride.

Intensity data were collected on a Picker four-circle automatic diffractometer equipped with a graphite monochromator using Mo $K\alpha$ radiation at a takeoff angle of 1.2°. A $\theta$-$2\theta$ scan mode over the range $3° < 2\theta \leq 50°$ at the rate of 1°/min with 20-s stationary-counter stationary-crystal background counts at both ends of the scan was used to collect a total of 3374 reflections in the $hkl$ octant. Of these, 2142 reflections having $F^2 > 3\sigma(F^2)$ were used in the solution and refinement of the structure. As a general check on electronic and crystal stability the intensities of three standard reflections were recorded at intervals of 100 reflections; no significant variation in intensity was observed during the data collection period for the three standards monitored. The data were processed using the formula of Ibers and co-workers[15] for the estimated standard deviation $\sigma(I) = [C + 0.25(t_s/t_b)^2(B_H + B_L) + p^2I^2]^{1/2}$; the value of $p$ was assigned as 0.05.[16] The values of $I$ and $\sigma(I)$ were corrected for Lorentz-polarization effects using the expression[17]

$$\frac{1}{Lp} = \frac{2 \sin 2\theta}{\cos^2 2\theta_m + \cos^2 2\theta}$$

where $\theta_m$, the angle of the monochromator, was 12.0°. In view of the crystal dimensions and the very small attenuation coefficient for $[Ru(py)_6](BF_4)_2$ (Mo $K\alpha$ radiation, $\mu$ = 5.6 cm$^{-1}$) the data were not corrected for absorption.

**Solution and Refinement of the Crystal Structure.** Examination of a three-dimensional Patterson function yielded the position of the ruthenium atom, and two cycles of least-squares refinement were carried out on this position. All least-squares refinements in this study were carried out on $F$, the function minimized being $\Sigma w(|F_o| - |F_c|)^2$ where the weight, $w$, is taken as $4F_o^2/\sigma^2(F_o^2)$. When calculating $F_c$, the atomic scattering factors for nonhydrogen atoms were taken from ref 18a. The effects of anomalous dispersion of Ru were also included in the calculation of $F_c$; the values of $\Delta f'$ and $\Delta f''$ again were taken from ref 18b. The remaining nonhydrogen atoms were located from a difference Fourier synthesis, and isotropic least-squares refinement of these positions yielded values of the conventional residuals $R_1$ = 0.115 and $R_2$ = 0.144, where $R_1 = \Sigma(|F_o| - |F_c|)/\Sigma|F_o|$ and $R_2 = [\Sigma w(|F_o| - |F_c|)^2/w(F_o)^2]^{1/2}$; anisotropic refinement of Ru, N, and F atoms led to final values of $R_1$ = 0.063 and $R_2$ = 0.075. No correction for secondary extinction was necessary.

In the final cycle of least-squares refinement, no atom parameter shifted by more than 0.20 times its estimated standard deviation, indicating that refinement had converged. The value of $R_2$ showed no unusual dependence on $|F|$ or sin $\theta$, indicating that our weighting scheme was appropriate. In the final difference Fourier synthesis there was no peak higher than 0.60 e Å$^{-3}$. The positional and thermal parameters for $[Ru(py)_6][BF_4]_2$ are listed in Tables I and II; observed and calculated structure amplitudes are available.

## Results and Discussion

**Synthesis of $[Ru(py)_6][BF_4]_2$.** Hexakis(pyridine)ruthenium(II) salts have been reported previously as precursors to tetrapyridine derivatives, but no preparative details were published at that time.[19] We have found that the $Ru(py)_6^{2+}$ cation is formed upon prolonged reflux of $[RuH(H_2O)_2(MeOH)(PPh_3)_2][BF_4]$ in methanol with excess pyridine. The solvated ruthenium(II) hydride starting material is only slightly soluble in methanol, and the progress of the reaction can be monitored by observing the disappearance of the solid reactant which is accompanied by darkening of the initial yellow solution to a deep orange. The $[Ru(py)_6][BF_4]_2$ product precipitates from the hot filtrate upon cooling. Slow crystallization of the desired salt to form large single crystals was promoted by the addition of methanol to the methanol–pyridine mother liquor followed by allowing the two phases to mix by diffusion over a period of several days.

The product was shown to be a 2:1 electrolyte by conductivity measurements in nitromethane. A molar conductivity of 158 $\Omega^{-1}$ cm$^2$ mol$^{-1}$ at a concentration of $1.12 \times 10^{-3}$ M is well within the range of 150–180 $\Omega^{-1}$ cm$^2$ mol$^{-1}$ considered appropriate for 2:1 electrolytes in nitromethane.[14] Further confirmation of the ionic species present in solutions of $[Ru(py)_6][BF_4]_2$ was obtained from a plot of the equivalent conductivity vs. the square root of the equivalent concentration according to the method of Feltham and Hayter.[20] The equivalent conductivity at each of five concentrations was determined by the equation

**Table I.** Final Atomic Positional and Isotropic Thermal Parameters for $[Ru(NC_5H_5)_6][BF_4]_2$[a]

| atom | x | y | z | B, Å² |
|---|---|---|---|---|
| Ru | 0.115 48(5) | 0.221 40(8) | 0.250 00 | |
| N(1) | 0.1883(7) | 0.0892(9) | 0.3045(7) | |
| N(2) | 0.0390(7) | 0.3562(10) | 0.2011(7) | |
| N(3) | 0.1931(7) | 0.3681(9) | 0.2899(6) | |
| N(4) | 0.0431(7) | 0.0767(11) | 0.2035(6) | |
| N(5) | 0.1830(6) | 0.2113(10) | 0.1523(6) | |
| N(6) | 0.0449(7) | 0.2304(10) | 0.3462(6) | |
| 1C(1) | 0.220(1) | −0.016(1) | 0.274(1) | 2.6(2) |
| 1C(2) | 0.273(1) | −0.096(1) | 0.309(1) | 4.5(3) |
| 1C(3) | 0.295(1) | −0.066(2) | 0.380(1) | 4.9(3) |
| 1C(4) | 0.261(1) | 0.040(1) | 0.415(1) | 4.4(3) |
| 1C(5) | 0.212(1) | 0.113(1) | 0.376(1) | 3.4(3) |
| 2C(1) | −0.040(1) | 0.339(1) | 0.208(1) | 3.9(3) |
| 2C(2) | −0.094(1) | 0.425(1) | 0.176(1) | 4.5(3) |
| 2C(3) | −0.067(1) | 0.527(2) | 0.137(1) | 5.6(4) |
| 2C(4) | 0.013(1) | 0.549(2) | 0.131(1) | 5.7(4) |
| 2C(5) | 0.065(1) | 0.458(1) | 0.165(1) | 4.3(3) |
| 3C(1) | 0.269(1) | 0.345(1) | 0.293(1) | 4.1(3) |
| 3C(2) | 0.325(1) | 0.432(2) | 0.316(1) | 5.0(3) |
| 3C(3) | 0.299(1) | 0.551(2) | 0.338(1) | 5.7(4) |
| 3C(4) | 0.219(1) | 0.582(1) | 0.334(1) | 4.7(3) |
| 3C(5) | 0.169(1) | 0.482(1) | 0.310(1) | 4.2(3) |
| 4C(1) | 0.008(1) | 0.099(2) | 0.140(1) | 4.7(4) |
| 4C(2) | −0.044(1) | 0.007(2) | 0.105(1) | 5.6(4) |
| 4C(3) | −0.059(1) | −0.103(2) | 0.142(1) | 6.3(4) |
| 4C(4) | −0.021(1) | −0.131(2) | 0.208(1) | 6.1(4) |
| 4C(5) | 0.031(1) | −0.040(1) | 0.236(1) | 4.0(3) |
| 5C(1) | 0.229(1) | 0.315(1) | 0.131(1) | 3.8(3) |
| 5C(2) | 0.276(1) | 0.311(1) | 0.066(1) | 4.6(3) |
| 5C(3) | 0.280(1) | 0.198(2) | 0.026(1) | 5.3(4) |
| 5C(4) | 0.234(1) | 0.095(2) | 0.048(1) | 4.7(3) |
| 5C(5) | 0.187(1) | 0.106(1) | 0.109(1) | 3.3(3) |
| 6C(1) | 0.028(1) | 0.123(1) | 0.385(1) | 3.6(3) |
| 6C(2) | −0.021(1) | 0.118(1) | 0.447(1) | 4.5(3) |
| 6C(3) | −0.055(1) | 0.233(2) | 0.468(1) | 5.5(4) |
| 6C(4) | −0.038(1) | 0.342(2) | 0.430(1) | 5.7(4) |
| 6C(5) | 0.009(1) | 0.337(2) | 0.369(1) | 4.3(3) |
| B(1) | 0.231(1) | 0.726(2) | 0.109(1) | 4.9(4) |
| B(2) | 0.012(1) | 0.740(2) | 0.417(1) | 5.5(4) |
| 1F(1) | 0.166(1) | 0.797(1) | 0.120(1) | |
| 1F(2) | 0.216(1) | 0.614(1) | 0.101(1) | |
| 1F(3) | 0.266(2) | 0.766(2) | 0.044(1) | |
| 1F(4) | 0.279(1) | 0.762(2) | 0.157(1) | |
| 2F(1) | 0.075(1) | 0.818(1) | 0.411(1) | |
| 2F(2) | −0.047(1) | 0.802(2) | 0.405(2) | |
| 2F(3) | 0.015(2) | 0.646(2) | 0.373(2) | |
| 2F(4) | 0.010(2) | 0.619(3) | 0.477(2) | |

[a] Numbers in parentheses are the estimated standard deviations of the coordinates and refer to the last significant digit of the preceding number.

$$\Lambda_e = \frac{k}{C_e}(L - L_s) \quad (1)$$

where $\Lambda_e$ is the equivalent conductance, $k$ is the cell constant, $L$ is the solution conductivity, $L_s$ is the pure solvent conductivity, and $C_e$ is the equivalent concentration which is based on an equivalent weight equal to the mass in grams per equivalent of the mononegative tetrafluoroborate anion as deduced from elemental analysis results. A plot of $\Lambda_0 - \Lambda_e$ vs. $C_e^{1/2}$ was made after $\Lambda_0 = 115\ \Omega^{-1}\ cm^2\ equiv^{-1}$ was obtained by extrapolation of a plot of $\Lambda_e$ vs. $C_e^{1/2}$ to infinite dilution. The slope of 640 for $\Lambda_0 - \Lambda_e$ vs. $C_e^{1/2}$ can be compared with values reported by Feltham and Hayter for 1:1, 2:1, and 3:1 electrolytes in nitromethane as near 200, 500, and 1000, respectively.[20] Some variation for the slope within a group of similar electrolytes is expected since the slope is a function of $\Lambda_0$.

**NMR Properties of $[Ru(py)_6][BF_4]_2$.** The resolution of $^1H$ and $^{13}C$ signals which were observed in acetonitrile-$d_3$ indicated that no paramagnetic species were present, and a formulation based on a ruthenium(II) $d^6$ complex was deemed appropriate. No $^1H$ resonance was observed above the acetonitrile solvent signal in the high-field region appropriate for a ruthenium hydride signal. Furthermore, no triphenylphosphine was present as evidenced by NMR, IR, and analytical data (vide infra). The data suggested that the solid isolated was indeed a simple hexakis(pyridine)ruthenium(II) tetrafluoroborate salt. The X-ray structure which was subsequently determined confirmed this formulation.

Chemical-shift data for $^1H$ and $^{13}C$ nuclei are presented in Table III. The pyridine resonances indicate that all of the ligands are magnetically equivalent on the NMR time scale. This is evident in the $^1H$ data, but it is seen more easily in the $^{13}C$ spectrum where a clean three-line pattern correlates with the spectrum predicted for the ortho, meta, and para carbon atoms of six NMR equivalent pyridine ligands. Assignments for both the $^1H$ and $^{13}C$ resonances for complexed pyridine were unambiguous. Recent data presented by Lavallee, Baughman, and Phillips for ortho-deuterated pyridine complexes[21] has confirmed the validity of the generally accepted ortho, meta, and para chemical shift ranges for both hydrogen and carbon nuclei of pyridine ligands.

Interpretation of the proton chemical shifts in terms of the interaction between ruthenium and pyridine must necessarily be limited in scope. The ortho protons are shifted most upon coordination ($\Delta\delta_o = -0.48$ ppm, i.e., shifted upfield by coordination) while the meta protons are only weakly influenced ($\Delta\delta_m = +0.10$ ppm) and the para proton chemical shift response is intermediate ($\Delta\delta_p = +0.30$ ppm). Comparison with $^1H$ NMR data reported by Raichart and Taube for $Ru(py)_4X_2$ (X = Cl, Br, and I; both cis and trans isomers were studied for each complex)[22] reveals a consistent trend as one considers the chemical shift of the pyridine ortho protons in the series with X = py representing the limiting $Ru(py)_6^{2+}$ formulation reported here. The order of the ortho proton chemical shifts is I < Br < Cl < py, which can be correlated with the total electron density present on the donor atom X. Thus one could conclude that the factor responsible for the order of the observed shifts is the diamagnetic contribution from orbitals remote from the ortho proton, in this case caused by electron circulation about the halide ligand X. In terms of the shielding parameters discussed by Meester, Stufkens, and Vrieze[23] the $\sigma_d'$ term would be expected to vary with X while the local diamagnetic contribution ($\sigma_d$) would be influenced less directly by ligand substitution at the ruthenium(II) center. The local paramagnetic term ($\sigma_p$) is unimportant for protons and the remote paramagnetic term ($\sigma_p'$) is expected to be relatively constant owing to the inverse dependence on the energies of the ligand field transitions,[24] all of which occur at relatively high energy in these complexes.

An alternative explanation based on simple electronegativity concepts is not adequate since the reverse order would be predicted, i.e., the $Ru(py)_3I_2$ fragment should be less electrophilic than $Ru(py)_3Br_2$ and hence greater electron withdrawal from the pyridine in the sixth position should lower the ortho proton chemical shift more in the bromide than the iodide; this is contrary to the experimental results.

Another possible chemical shift rationale involving bond anisotropies between the metal and ligand X would seem inadequate since halide ligands can only form double bonds via donation of $\pi$ electrons and not via acceptance of $\pi$ electrons. Here the ruthenium $d^6$ ion has the $d\pi$ orbitals filled and hence no halide $p\pi$ donation will occur and no double-bond character is expected in the Ru–X system for X = Cl, Br, or I.

The slight downfield shift which occurs for the meta and para protons upon coordination of pyridine to ruthenium is probably due to a withdrawal of electron density from the aromatic ring as a result of the dative bond from nitrogen to the

**Table II.** Final Anisotropic Thermal Parameters ($\times 10^3$) for $[Ru(NC_5H_5)_6][BF_4]_2$[a]

| atom | $\beta_{11}$ | $\beta_{22}$ | $\beta_{33}$ | $\beta_{12}$ | $\beta_{13}$ | $\beta_{23}$ |
|---|---|---|---|---|---|---|
| Ru | 2.72(3) | 4.74(7) | 2.33(3) | −0.14(5) | 0.19(6) | −0.25(12) |
| N(1) | 2.9(5) | 5.9(11) | 3.3(4) | −0.3(6) | −0.6(4) | −0.4(6) |
| N(2) | 3.1(5) | 5.7(11) | 2.9(4) | 0.6(6) | −0.2(4) | −0.6(5) |
| N(3) | 3.0(5) | 4.8(10) | 2.7(4) | 0.2(6) | −0.1(3) | −1.2(5) |
| N(4) | 2.0(5) | 9.1(13) | 2.9(4) | −0.4(6) | 0.2(4) | −0.5(6) |
| N(5) | 3.0(4) | 5.9(10) | 2.5(4) | −0.2(6) | −0.2(3) | −0.1(6) |
| N(6) | 3.8(5) | 5.0(9) | 2.7(4) | 0.2(6) | −0.4(4) | −0.7(6) |
| 1F(1) | 8(1) | 28(2) | 11(1) | 3(1) | −3(1) | −6(1) |
| 1F(2) | 19(2) | 12(1) | 22(2) | −4(1) | 14(2) | −2(1) |
| 1F(3) | 21(2) | 23(2) | 9(1) | −8(2) | 4(1) | −3(1) |
| 1F(4) | 8(1) | 67(5) | 10(1) | 8(2) | −4(1) | −15(2) |
| 2F(1) | 11(1) | 16(2) | 19(2) | −3(1) | −7(1) | 6(1) |
| 2F(2) | 7(1) | 29(3) | 26(2) | 4(1) | −4(1) | −2(2) |
| 2F(3) | 22(2) | 17(2) | 27(2) | −8(2) | 15(2) | −15(2) |
| 2F(4) | 30(4) | 68(8) | 18(2) | −14(5) | −9(3) | 24(4) |

[a] The form of the anisotropic temperature factor expression is $\exp[-2\pi^2(\beta_{11}h^2a^{*2} + \beta_{22}k^2b^{*2} + \beta_{33}l^2c^{*2} + 2\beta_{12}hka^*b^* + 2\beta_{13}hla^*c^* + 2\beta_{23}klb^*c^*)]$.

**Table III.** NMR Data for $[Ru(py)_6][BF_4]_2$ and Related Pyridine Derivatives

| complex | $\delta^1$H(ortho)[a] | $\delta^1$H(meta) | $\delta^1$H(para) | solvent | ref |
|---|---|---|---|---|---|
| $[Ru(py)_6]^{2+}$ | 8.02 d | 7.30 t | 7.90 t | $CD_3CN$ | this work |
| *trans*-$Ru(py)_4Cl_2$ | 8.60 d | 7.05 t | 7.61 t | $CDCl_3$ | 22 |
| *trans*-$Ru(py)_4Br_2$ | 8.74 d | 7.06 t | 7.63 t | $CDCl_3$ | 22 |
| *trans*-$Ru(py)_4I_2$ | 9.01 d | 7.01 t | 7.63 t | $CDCl_3$ | 22 |
| *cis*-$Ru(py)_4Cl_2$ | 8.68 d<br>8.35 d | 7.12 q | 7.63 q | $CDCl_3$ | 22 |
| *cis*-$Ru(py)_4Br_2$ | 8.89 d<br>8.40 d | 7.13 q | 7.66 q | $CDCl_3$ | 22 |
| *cis*-$Ru(py)_4I_2$ | 9.08 d<br>8.42 d | 7.11 q | 7.63 q | $CDCl_3$ | 22 |
| $[Ru(py)(NH_3)_5]^{2+}$ | 8.45 d | 7.3 t | 7.75 t | $D_2O$ | 24 |
| py | 8.50 | 7.20 | 7.60 | $CH_3CN$ | this work |
| py | 8.66 | 7.29 | 7.70 | $CDCl_3$ | 22 |
| py | 8.61 | 7.35 | 7.79 | $CD_3COCD_3$ | *b* |
| py | 8.66 | 7.20 | 7.61 | $C_6H_{12}$ | 25 |
| $Hpy^+$ | 8.91 | 8.26 | 8.83 | $CF_3CO_2H$ | 25 |
| py | 8.60 | 7.48 | 7.91 | $D_2O$ | *b* |
| py | 6.73 | 5.59 | 6.01 | $D_2O$ relative to $C_6H_{12}$ | *c* |
| $Hpy^+$ | 7.33 | 6.59 | 7.13 | $D_2O$ relative to $C_6H_{12}$ | *c* |
| complex | $\delta^{13}$C(ortho) | $\delta^{13}$C(meta) | $\delta^{13}$C(para) | solvent | ref |
| $[Ru(py)_6]^{2+}$ | 155.9 | 125.2 | 137.3 | $CD_3CN$ | this work |
| py | 150.6 | 124.6 | 136.6 | $CD_3CN$ | this work |
| py | 150.2 | 123.9 | 135.9 | | 26 |
| $Hpy^+$ | 142.4 | 129.0 | 148.3 | | 26 |

[a] The $^1$H spectrum of free and coordinated pyridine is quite complex with considerable fine structure. However, it is possible to identify crude doublets (d) and triplets (t) which can be associated with the various types of protons present as has been done by Raichart and Taube.[22] [b] R. J. Chuck and E. W. Randall, *J. Chem. Soc. B*, 261 (1967). [c] J. B. Merry and J. H. Goldstein, *J. Am. Chem. Soc.*, **88**, 5560 (1966).

metal. A downfield shift of all the aromatic pyridine protons, including the ortho proton, is observed when pyridine is protonated ($\Delta\delta_o$ = +0.25 ppm, $\Delta\delta_m$ = +1.06, $\Delta\delta_p$ = +1.22).[25] The $^1$H chemical shifts can be compared with data reported by Lavallee and Fleischer for the $(NH_3)_5Ru(py)^{2+}$ cation.[24] Following a thorough discussion of the NMR spectra of several pentaammineruthenium(II) complexes with aromatic ligands it was concluded that the diamagnetic shifts of the para and meta protons were indicative of an overall polarization of electron density toward the ruthenium(II) ion upon coordination. The role of $d\pi$–$p\pi$ back-bonding from the $d^6$ metal ion was at most a secondary factor since the observed downfield shifts for the para and meta positions were inconsistent with increased $\pi$ (or $\pi^*$) electron density at these sites.

The paramagnetic anisotropy of the ruthenium(II) center ($\sigma_p'$) may produce either an upfield or a downfield shift. The upfield shift observed for the pyridine ortho protons in $[(NH_3)_5Ru(py)]^{2+}$ ($\Delta\delta_o$ = −0.15 ppm) has been attributed to the temperature-independent paramagnetic anisotropy of the $d^6$ metal ion.[24] The upfield shift observed for the ortho protons of $[Ru(py)_6]^{2+}$ can be explained by invoking a similar mechanism. The $(NH_3)_5Ru(py)^{2+}$ NMR data are consistent with the above discussion where the $\sigma_d'$ factor determines the order of the ortho $^1$H chemical shifts for pyridine bound to ruthenium(II). The electron density associated with coordinated ammonia will be less than that of any of the halides; hence the $\sigma_d'$ diamagnetic contribution is less and a net upfield shift is observed as $\sigma_p'$ dominates. Furthermore, the upfield shift at the ortho position of $(NH_3)_5Ru(py)^{2+}$ is less than that of $(py)_5Ru(py)^{2+}$ as would be predicted. Although the coordinated atoms of the ligands cis to pyridine are nitrogens in both cases, only for $(py)_5Ru(py)^{2+}$ will the ortho protons set in the field of an aromatic ring for certain rotamers. Examination of the geometric parameters of the $Ru(py)_6^{2+}$ ion

**Table IV.** Infrared Data for $[Ru(py)_6][BF_4]_2$

| $\nu$, $cm^{-1}$ | assignment[a] | $\nu$, $cm^{-1}$ | assignment[a] |
|---|---|---|---|
| 3140 w[b] | py | 1159 s | py ($\nu$15) |
| 3080 w | py | 1080 vvs | $BF_4^-$($\nu$3) |
| 1603 m | py ($\nu$8a) | 1055 vvs | $BF_4^-$ ($\nu$3) |
| 1570 w | py ($\nu$8b) | 1030 vvs | $BF_4^-$ ($\nu$3) |
| 1555 w | py ($\nu$8b) | 870 vw | py |
| 1482 m | py ($\nu$19a) | 769 s | py ($\nu$4) |
| 1475 sh | py ($\nu$19a) | 759 s | py ($\nu$4) |
| 1445 s | py ($\nu$19b) | 720 s | py ($\nu$11) |
| 1440 sh | py ($\nu$19b) | 708 s | py ($\nu$11) |
| 1385 m | py ($\nu$14) | 700 s | py ($\nu$11) |
| 1350 w | py ($\nu$6a + 10b) | 655 vw | py ($\nu$6b) |
| 1288 w | py | 520 m | $BF_4^-$ ($\nu$4) |
| 1236 w | py | 472 w | py ($\nu$16b) |
| 1220 w | py ($\nu$9a) | 326 vvw | Ru-N |
| 1212 sh | py ($\nu$9a) | | |

[a] The assignments suggested here are based on correlations between free and complexed pyridine presented in ref 28. [b] All data were obtained from Nujol mull spectra. Abbreviations: s, strong; m, medium; w, weak; sh, shoulder; v, very.

clearly indicates that the effect of this interaction will be a shielding of the proton by the adjacent pyridine ligands since the ortho protons lie in the shielding cone of a cis aromatic ligand.

Complexation of pyridine to the pentaammineruthenium(II) moiety has qualitatively the same effect on the para-proton chemical shift as does coordination to the pentapyridineruthenium(II) moiety.[24] This tends to confirm a minor role for $d\pi$-$p\pi$ back-bonding in determining this chemical shift since the ammine ligands remove none of the electron density from the ruthenium $t_{2g}$ orbitals while in the $Ru(py)_6^{2+}$ ion each pyridine would be expected to compete equally for the six $d\pi$ electrons. Hence the lowest $\pi^*$ orbital of pyridine in $(NH_3)_5Ru(py)^{2+}$ must have at least as much electron density as the same $\pi^*$ orbital in one of the pyridines of $Ru(py)_6^{2+}$ (indeed chemical intuition suggests that it would have more), yet the chemical shifts at the para position, often considered the most reliable indication of $\pi$-electron density, are experimentally within the range of solvent effects which have been reported.[21] To the extent that one can comment on the small difference observed the trend indicates less back-bonding per pyridine in the $Ru(py)_6^{2+}$ complex, as one would expect.

The $^{13}C$ chemical shift values are all decreased relative to free pyridine with the ortho carbon shifting most. Since the importance of the local paramagnetic term ($\sigma_p$) in $^{13}C$ NMR precludes even a qualitative discussion of the electronic origin of the shift behavior, suffice it to note that the ortho carbon shifts upfield while the para carbon undergoes a large downfield shift upon protonation of pyridine[26] in contrast to the $^{13}C$ chemical shift behavior observed upon coordination of six pyridine ligands to ruthenium(II). Comparison with the $^{13}C$ chemical shift data reported for the para carbon of a series of pyridine complexes[21] clearly places $Ru(py)_6^{2+}$ in the category of $\pi$ back-bonding coordination compounds, although the extent of donation from the metal to any individual pyridine is less than that characterizing the $(NH_3)_5Ru(py)^{2+}$ moiety, again in accord with chemical expectations.

Spectra have been recorded at temperatures as low as −40 °C with no observable change in multiplicity or line width for the three $^{13}C$ signals. From these data we conclude that the six pyridine ligands are equivalent on the NMR time scale either by molecular equivalence in solution or by rapid rotations of the planar pyridine ligands around the metal–nitrogen axis.

**Infrared Data.** The infrared spectrum of $[Ru(py)_6][BF_4]_2$ from 2000 to 700 $cm^{-1}$ (see Table IV for a compilation of observed frequencies) reproduces the vibrational bands of free pyridine with only minor shifts in positions, splittings, and intensities. The free pyridine band at 1578 $cm^{-1}$ (assigned as $\nu$8a in the notation of Kline and Turkevich[27]) is shifted to 1603 $cm^{-1}$ upon complexation to the ruthenium(II) ion; this sharp, distinct absorption near 1600 $cm^{-1}$ is a characteristic feature of infrared spectra of coordinated pyridine.

A number of ligand bands are split in the solid-state infrared spectrum of $[Ru(py)_6][BF_4]_2$. Comparison with representative spectra of coordinated pyridine as reported by Gill, Nuttall, Scaife, and Sharp[28] indicates that splitting has occurred to produce two bands for $\nu$8b (1570, 1555 $cm^{-1}$), $\nu$19a (1482, 1475), $\nu$19b (1445, 1440), $\nu$9a (1220, 1212), $\nu$4 (769, 759) and $\nu$11 (720, 708, and 700). Assessment of the observed splittings in terms of the molecular geometry is tempting in view of the solid-state structure as observed by X-ray crystallographic techniques (vide infra). However, one cannot eliminate interactions in the solid-state lattice as sources of the observed splitting. Hence no firm conclusions regarding variations in metal–ligand bonding can be derived from the solid-state vibrational data.

The similarity observed among infrared spectra of a number of pyridine complexes representing a variety of metals, oxidation states, and geometries has been interpreted as reflecting a relatively constant electron distribution in the ligand which can be rationalized in terms of back-bonding from the metal to the pyridine ligand.[28] The spectral details for the hexakis(pyridine)ruthenium(II) cation are consistent with this model.

Of particular interest in the infrared spectrum is the low-frequency region from 700 to 200 $cm^{-1}$. The two low-energy ring vibrations of free pyridine ($\nu$16b at 405 $cm^{-1}$ and $\nu$6a at 604 $cm^{-1}$) both respond to coordination of the pyridine and shift to higher frequency with the magnitude of the shift dependent on the oxidation state of the metal, the metallic radius, and the stereochemistry of the resultant complex.[29] Values typically range from 630 to 640 $cm^{-1}$ for $\nu$6a in pyridine complexes of the first-row transition metals while $\nu$16b varies from ca. 420 to 440 $cm^{-1}$ in such cases. Clark and Williams noted that both bands are shifted further (645 to 660 $cm^{-1}$ for $\nu$6a and 465 to 480 $cm^{-1}$ for $\nu$16b) and are less intense in pyridine complexes of second- and third-row transition metals.[29]

The four bands observed between 700 and 200 $cm^{-1}$ in the infrared spectrum of $[Ru(py)_6][BF_4]_2$ can be assigned with confidence based on the above considerations and two additional pieces of information: (1) the $BF_4^-$ ion exhibits an infrared-allowed bending mode as a weak absorption near 525 $cm^{-1}$;[30] (2) metal–pyridine stretching vibrations for heavy metal complexes are generally found in the region from 230 to 300 $cm^{-1}$ [29] with tetrakis(pyridine)dihaloruthenium(II) compounds favoring the high-energy portion of this range, i.e., the Ru–py stretching modes have been assigned near 300 $cm^{-1}$ for *cis*- and *trans*-$Ru(py)_4X_2$ with the X = Cl, Br, and I.[22]

Weak absorptions at 655 and 472 $cm^{-1}$ are separated by a band of medium intensity at 520 $cm^{-1}$ which is assignable as the bending mode of the tetrafluoroborate anion. The assignment of $\nu$6a to the 655-$cm^{-1}$ band implies a frequency shift of ca. 50 $cm^{-1}$ while $\nu$16b at 472 $cm^{-1}$ is 67 $cm^{-1}$ above the free pyridine frequency. These shifts support the generalization above regarding the observed dependence of these bands on the metal ion.[29]

The most incisive infrared absorption arises from the ruthenium–pyridine stretching mode of $T_{1u}$ symmetry. This band is infrared active and provides a direct and apodictic appraisal of the metal–ligand bonding in this octahedral complex. Even though this normal vibration is electronic dipole allowed it is *extremely* weak, and it is in fact easily overlooked except when very dense samples are examined. As can be seen in Figure 1 there is only one absorption between 200 and 450

$cm^{-1}$, and hence this weak infrared band at 326 $cm^{-1}$ can be confidently assigned as the $T_{1u}$ Ru-N stretching mode absorption. This assignment is consistent with the data cited above regarding previously reported ruthenium-pyridine vibrational frequencies. Extremely weak infrared absorptions have been assigned as the allowed $T_{1u}$ stretching band in other octahedral coordination complexes.[31]

The pseudooctahedral symmetry of the hexakis(pyridine)-ruthenium(II) cation allows one to calculate a ratio of ruthenium-nitrogen bond stretching force constants for $Ru(py)_6^{2+}$ and $Ru(NH_3)_6^{3+}$. Assuming that the nitrogenous ligands can be considered rigid units relative to the metal-nitrogen stretching mode enables one to apply a simple $MX_6$ vibrational analysis, where the effective mass of X is simply the molecular weight of the ligand. Although the two $T_{1u}$ vibrational symmetry coordinates (one stretching mode and one bending mode) of $MX_6$ can have nonzero off-diagonal elements, the magnitude of $f_d$, the bond stretching force constant, is usually large enough to allow one to approximate the solution of interest from the complete vibrational secular equation as in the equation

$$m_x\lambda_3 = \left(1 + 2\frac{m_x}{m_M}\right)(f_d - \delta) \qquad (2)$$

This approximation follows from the expressions derived for the general octahedral case by Claassen.[32] Here $\delta$ is the interaction force constant between two trans M-X bonds and $\lambda_3 = 4\pi^2c^2\tilde{\nu}_3^2$. For the series of nine $MF_6$ molecules analyzed by Claassen the value of $\delta$ was always less than 10% of $f_d$, and in four of the cases it was actually less than 1% of $f_d$. Clearly then the $(f_d - \delta)$ term should provide a meaningful assessment of the metal-ligand bond in closely related octahedral systems even when the separate values of $f_d$ and $\delta$ are not explicitly extracted.

Rewriting eq 2 and deriving the ratio of force constants for the ruthenium pyridine and ruthenium ammine complexes leads to the equation

$$\frac{(f_d - \delta)_{py}}{(f_d - \delta)_{NH_3}} = \frac{m_{py}(m_{Ru} + 2m_{NH_3})}{m_{NH_3}(m_{Ru} + 2m_{py})}\frac{[\tilde{\nu}_3(py)]^2}{[\tilde{\nu}_3(NH_3)]^2} \qquad (3)$$

A value of 463 $cm^{-1}$ can then be utilized for the hexaammineruthenium(III) cation[33] and a value of 326 $cm^{-1}$, based on the infrared assignments discussed above, for the ruthenium(II) pyridine counterpart. The resultant ratio $(f_d - \delta)_{py}/(f_d - \delta)_{NH_3}$ is equal to 1.20.

It has been effectively argued that the interaction force constants in $Ru(NH_3)_6^{3+}$ are small since coupling effects will be limited to $\sigma$ bonds and the mass of the central atom is large.[33] This logic guides one to conclude that the $\delta/f_d$ ratio for the pyridine complex will be greater than the corresponding ratio for the ammine analogue. The above comparison of force constants, which indicates that the ruthenium(II) pyridine $(f_d - \delta)$ term is 20% larger than the analogous ruthenium(III) ammine term, should then be equally valid with respect to direct comparison of the Ru-N force constants ($f_d$), and to the extent that the $\delta$ values are not negligible one would anticipate only further reinforcement of the above conclusion, i.e., the $Ru^{2+}$-py force constant exceeds the $Ru^{3+}$-$NH_3$ force constant.

A second ratio of interest would result from comparison between the two known octahedral ruthenium(II) cations, $Ru(py)_6^{2+}$ and $Ru(NH_3)_6^{2+}$. A definitive $\nu_3$(Ru-N) assignment has not yet been accepted in the literature (a value of 437 $cm^{-1}$ has been reported[34] and later refuted[35] while most M-N stretching vibrations for $M(NH_3)_6^{2+}$ complexes lie in the range of 300-330 $cm^{-1}$ [31]). If one assumes that $\nu_3$ for $Ru(NH_3)_6^{2+}$ is 300 $cm^{-1}$ (as was done by Stynes and Ibers[36]), a ratio of 2.86 is calculated for $[(f_d - \delta)_{py}/(f_d - \delta)_{NH_3}]$ from eq 3. Even when the calculation is based on the anomalously high 437-$cm^{-1}$ assignment for $\nu_3$,[34] a ratio considerably greater than one (1.35) results. It seems clear that the metal-ligand stretching force constant is greater for $Ru(py)_6^{2+}$ than for either $Ru(NH_3)_6^{3+}$ or $Ru(NH_3)_6^{2+}$.

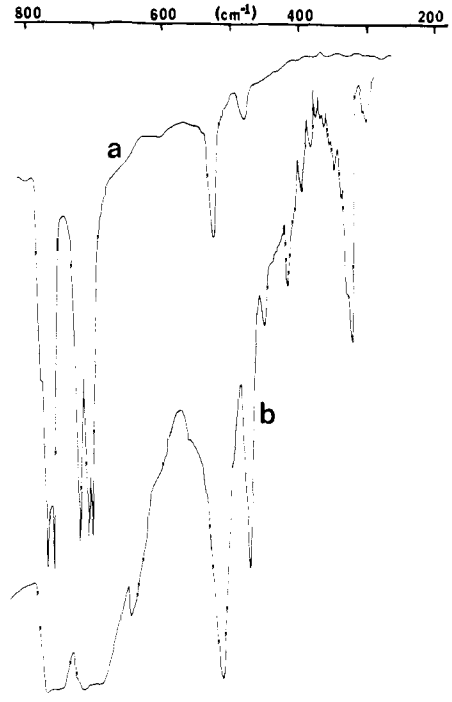


**Figure 1.** Infrared spectra of $[Ru(py)_6][BF_4]_2$ in the 200-800-$cm^{-1}$ region: (a) regular Nujol mull; (b) extremely thick Nujol mull displaying the 326-$cm^{-1}$ band.

Force constants are often considered a measure of bond strength, albeit the correlation is not always a simple one. An unusual set of circumstances obtains for the two octahedral cations, $Ru(py)_6^{2+}$ and $Ru(NH_3)_6^{3+}$, with respect to comparative bond strengths as reflected in the ratio of the respective stretching force constants and in the ruthenium-nitrogen bond distances as determined by X-ray crystallography. The shorter bond (2.104 (4) Å for Ru(III)-$NH_3$[36] vs. an average of 2.12 (1) Å for the six crystallographically distinct Ru(II)-py separations (see Table VIII)) seems to be the weaker of the two based on the ratio of force constants. The length of the Ru-py bonds may well be limited by steric repulsions among the six ligands which prohibit closer approach to the metal center.

Although it is generally true that a monotonic relationship exists between bond strength and bond length, the apparent paradox in the present case can be rationalized on the basis of both $\sigma$ and $\pi$ bonding interactions in the pyridine complex while the hexaammineruthenium(III) will be held together by $\sigma$-only bonds. Evidently the total constructive overlap stabilizing the ruthenium-nitrogen bond is greater in the pyridine case as the $d^6$ metal center provides electron density for the $\pi$ Ru-N interaction to complement the normal dative metal-ligand $\sigma$ bond. In spite of widespread acceptance of the concept of retrodative bonding it is seldom as demonstrable as in the present case where the same metal atom-donor atom moiety is differentiated in two complexes by a unique combination of $\pi$ back-bonding and steric control of the Ru-N distance in one of the two. The result based on molecular structure determinations and vibrational data is a *longer, stronger* bond for the nitrogenous ligand which has the potential to serve as a $\pi$ acid ligand.

**UV-Visible Spectra.** The electronic spectrum of $[Ru(py)_6][BF_4]_2$ in acetonitrile exhibits three distinct absorption maxima between 220 and 700 nm (see Table V). The 243-nm band is assigned as a pyridine localized $\pi \rightarrow \pi^*$ transition based

**Table V.** Electronic Absorption Data for $[Ru(py)_6][BF_4]_2$

| complex | $\lambda_{max}$, nm | $E \times 10^{-3}$, $cm^{-1}$ | $\epsilon \times 10^{-3}$, $M^{-1}$ $cm^{-1}$ | ref |
|---|---|---|---|---|
| $Ru(py)_6^{2+}$ | 341 | 29.3 | 22.8 | this work |
| | 272 | 36.8 | 5.7 | |
| | 243 | 41.2 | 22.8 | |
| $(NH_3)_5Ru(py)^{2+}$ | 407 | 24.5 | 7.8 | *a* |
| *cis*-$[(NH_3)_4Ru(py)_2]^{2+}$ | 410 | 24.4 | 7.9 | *b* |
| | 375 | 26.6 | 6.5 | |
| *trans*-$[(NH_3)_4Ru(py)_2]^{2+}$ | 423 | 23.6 | 16.6 | *b* |

[a] R. E. Hintze and P. C. Ford, *Inorg. Chem.*, **14**, 1211 (1975). [b] P. C. Ford and C. Sutton, *ibid.*, **8**, 1544 (1969).

on the position and intensity of this absorption which are compatible with parameters reported for such bands in free pyridine, protonated pyridine, and $[(NH_3)_5Ru(py)]^{n+}$.[37] In particular the $[(NH_3)_5Ru(py)]^{2+}$ cation displays a band at 244 nm with $\epsilon$ $4.6 \times 10^3$ $M^{-1}$ $cm^{-1}$ with a similar transition intensity characterizing $Ru(py)_6^{2+}$ when converted to a normalized absorption scale per mol of pyridine ligand rather than per mol of metal complex ($\epsilon_{py}$ 3800 $M^{-1}$ $cm^{-1}$ for $Ru(py)_6^{2+}$ at 243 nm; cf. 4600 $M^{-1}$ $cm^{-1}$ for $(NH_3)_5Ru(py)^{2+}$ at 244 nm). The analogous $\pi \rightarrow \pi^*$ transition in free pyridine, pyridinium cation, and $(NH_3)_5Ru(py)^{3+}$ occurs near 253 nm.

The intense low-energy band at 345 nm is assigned as a $d \rightarrow \pi^*$ metal-to-ligand charge transfer (MLCT) transition which produces an excited state crudely resembling ruthenium(III) and reduced pyridine. Similar MLCT bands are prominent in other ruthenium(II) complexes containing pyridine.[38] Such a transition originates from the filled metal $(d\pi)^6$ orbitals, and hence this electronic transition should be sensitive to factors which alter the energy of the metal orbitals while the empty $\pi^*$ energy level of the pyridine ligand would be expected to remain relatively constant from one complex to another.

Charge-transfer transitions provide direct information regarding the separation of molecular energy levels which are substantially localized on the metal and ligand, respectively. The interpretation of such data is not, however, as clear-cut as one might hope. Zwickel and Creutz have obtained molecular orbital parameters for $(NH_3)_5Ru(L)^{2+}$ and $(NH_3)_4Ru(L)_2^{2+}$ (both cis and trans isomers) based on a simple semiempirical method for analyzing the charge-transfer spectra of these compounds when L is a nitrogen heterocycle.[39] A series of logical assumptions reduce the orbitals considered to only the lowest lying pyridine $\pi^*$ orbital of $B_2$ symmetry in the free ligand and the single metal $t_{2g}$ type orbital which overlaps effectively with the $\pi^*$ acceptor orbital on the ligand. For $(NH_3)_5Ru(py)^{2+}$ the result is a two-orbital problem which is parametrized in terms of the energy difference between the hypothetical noninteracting metal and ligand orbitals of interest ($\delta = \alpha_L - \alpha_{Ru}$ where $\alpha_L = (\pi^*|H|\pi^*)$ and $\alpha_{Ru} = (t_{2g}|H|t_{2g})$) and the matrix element connecting these same orbitals ($\beta = (\pi^*|H|t_{2g})$). The orientation of the two pyridine ligands in both the cis and trans forms of $(NH_3)_4Ru(py)_2^{2+}$ is critical to the extension of this method to these tetraammine complexes. The assumption that the cis complex will exist with the pyridine ligands maintaining a vertical orientation within the *xz* and *yz* planes seems attractive with respect to steric considerations, although as a cautionary note it should be admitted than an *xz*, *xy* ligand orientation cannot rigorously

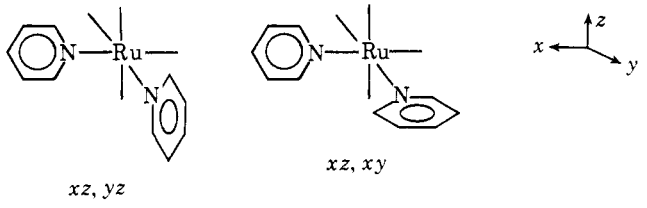


*xz*, *yz* *xz*, *xy*

be discounted on steric grounds since this is the arrangement found for cis pyridines in the $Fe(py)_6^{2+}$ cation.[9] The observation of two MLCT bands in the cis case can be rationalized by the *xz*, *yz* orientation which predicts two allowed transitions, one to the nonbonding $\pi^*$ combination and one to the antibonding $\pi^*$ plus $t_{2g}$ combination.

The trans case is somewhat more paradoxical in that the observation of one band at lower energy than in the monopyridinepentaammine complex seems inconsistent with the intuitive expectation that the additional pyridine will lower the metal orbital energies by increasing the effective nuclear charge of ruthenium and hence increase the energy gap which is traversed during the transition from $t_{2g}$ to $\pi^*$. The most crucial assumption in the Zwickel and Creutz analysis is that $\beta$ and $\delta$ remain constant for a given heterocycle,[39] and it is this assumption which deserves close examination. If one accepts the validity of this premise then it would follow, as the authors point out, that *trans*-$(NH_3)_4Ru(py)_2^{2+}$ would have the same MLCT spectra as the monopyridine complex if the two pyridine planes were orthogonal to one another since each pyridine would then interact independently with a separate $d\pi$ orbital. The spectral energy difference between the two cases would then result solely from an increase in effective nuclear charge. The authors conclude that the lower frequency observed for the MLCT transition in *trans*-$(NH_3)_4Ru(py)_2^{2+}$ relative to $(NH_3)_5Ru(py)^{2+}$ is incompatible with such an analysis while a trans geometry with coplanar pyridine ligands can account for this experimental result.

Rational estimates of the extent of metal-to-ligand $\pi$ back-bonding can be derived from spectral analysis and from potential measurements. According to Zwickel and Creutz the extent of $\pi$ interaction deduced from potential data is greater than that calculated from spectral data within the framework of their molecular orbital treatment.[39] A rationalization of this result was presented based on the increased effective charge on ruthenium(II) as pyridine replaces ammonia which results in a stabilization of both the ground state and the excited state. This effect is therefore not observable in the spectral energy, but does manifest itself in the electrochemical data where only the ground-state features of the energy difference between the ruthenium 2+ (stabilized by increased back-bonding) and 3+ (negligible $\pi$ stabilization) are measured. While the Zwickel and Creutz charge-transfer analysis has many commendable features, the final paragraph concludes that "back-bonding increases the effective charge on Ru(II)", yet as discussed above this will necessarily increase the $t_{2g}$, $\pi^*$ energy gap ($\delta$) in the hypothetical metal-ligand scheme prior to orbital interaction. This directly contradicts the assumption that $\beta$ and $\delta$ will remain constant for pyridine as the ruthenium ligand set varies.

The extension of this simple molecular orbital treatment to the $Ru(py)_6^{2+}$ cation cannot succeed within a framework based on a constant $\delta$ value. While it is possible to contend that such a premise would not be expected to prevail when six pyridines are bound to the ruthenium(II) center, one could assert that the maximum variation in $\delta$ per pyridine would exist for the $(NH_3)_{6-n}Ru(py)_n^{2+}$ pair with $n = 0, 1$. Certainly for the pair with $n = 0, 6$ the difference in the absolute energy of the metal $t_{2g}$ orbitals will be quite large and therefore of obvious importance in comparing spectral properties, but it also seems inappropriate to assume that $\delta$ will remain constant even for comparison of the $n = 1, 2$ pair of complexes. Although Zwickel and Creutz cite the proximity of ammonia and pyridine in the spectrochemical series as support for the assumption that $\delta$ and $\beta$ remain constant as $n$ varies from 1 to 2, it is well established that this similarity is only coincidental and in fact the ligand features that produce roughly equivalent d orbital splittings are very different for the unsaturated nitrogen heterocycle and the ammine ligand.

An alternative approach to the analysis of charge-transfer spectra in these complexes presents itself if one accepts the more realistic viewpoint that the limited data available severely limit the application of a simple quantitative theory to the observed transition energies. Furthermore, the extraction of constant $\beta$ and $\delta$ parameters for a given heterocycle is inconsistent with the qualitative features exhibited by ruthenium(II)pyridine complexes. It should be recognized at the outset that the following treatment is susceptible to a number of legitimate criticisms, but it is the author's belief that, taken in its entirety, it provides a more accurate description of the molecular properties under consideration than previous models.

It is a generally accepted fact that the effective charge on Ru(II) will increase as pyridines replace ammines in the coordination sphere. Of utmost importance to the following treatment is the realization that $\pi$ effects are invariably of secondary importance relative to $\sigma$ factors and hence a cancellation of $\sigma$ effects should obtain before data are interpreted on the basis of $\pi$ bonding. With regard to the charge at the metal center this tenet implies that the effective nuclear charge for *cis*-dipyridinetetraammineruthenium(II) will be greater than that of the trans complex regardless of the orientation of the planar pyridine ligands (i.e., the $\sigma$ effect on the metal charge, which is independent of the rotameric configuration, will be less in the trans case than in the cis case and this factor will be dominant). This feature is evident in the molecular structure of $\mu$-oxalato-bis(tetrapyridineruthenium(II))[19] where the Ru–N distances for the trans pyridines average 2.09 Å while the cis distances average 2.07 Å. The longer trans bond lengths persist in spite of the lack of competition for $\pi$ bonding to the same metal $t_{2g}$ orbital which is completely alleviated by the observed 81° angle between the normals of the two trans pyridine ligands.

The increase in nuclear charge at the metal center accompanying additional pyridines lowers the $t_{2g}$ energy levels prior to interaction with the ligand orbitals and therefore it would seem intuitively appealing that $\delta$ should increase with additional pyridine ligands. Indeed one would hope to build this feature into any proposed model.

The Zwickel and Creutz parameters $\beta$ and $\delta$ may be unambiguously extracted for a single complex only for *cis*-$(NH_3)_4Ru(py)_2^{2+}$ where two band maxima are experimentally observed.[39] The resultant values of $\delta = 22.2 \times 10^3$ cm$^{-1}$ and $\beta = 5.2 \times 10^3$ cm$^{-1}$ serve as a reference point for a semiquantitative assessment of $\beta$ and $\delta$ in other pyridineammine complexes of ruthenium(II).

The marriage of orbital energies based on optical transitions and molecular energies derived from potential measurements must be undertaken with some degree of reluctance. Even if one accepts the framework of approximations required it is still true that one measures a single orbital energy difference between the ground state and an excited-state configuration spectrally while the electrochemical information relates to a difference between the total energy of two complexes which differ not only by the addition or removal of one electron from a specific orbital, but also by a reorganization of all the molecular orbitals which are substantially altered by the redox process. Nonetheless it would seem reasonable to seek limited correlations between data obtained via these two diverse techniques.

A quantitative estimate of the stabilization energy resulting from $\pi$ back-bonding can be obtained from the charge-transfer spectrum molecular orbital parameters by subtracting the energy of the metal localized ($t_{2g} + \pi^*$) bonding orbital from that of the pure metal $t_{2g}$ orbital as was done by Zwickel and Creutz.[39] However, it should be noted that the calculated energy gap between perturbed and unperturbed d$\pi$ orbitals is not equal to the total stabilization energy realized which depends on a simple multiplicative factor equal to the number of electrons occupying the molecular orbitals. For the monopyridine case one $t_{2g}$ orbital mixes with the ligand $\pi^*$ orbital and hence the total energy change in the system should be twice that of the energy gap owing to the presence of two electrons in the orbital which is lowered. The spectral data thus guides one to a simple difference between perturbed and unperturbed $t_{2g}$ orbital energies. Interpretation of oxidation potential differences on this basis must invoke a factor of 2 relative to the spectral energy gap since the $\pi$ stabilization of two electrons per orbital is lost upon oxidation to Ru(III) based on the assumptions employed to allow comparison with data for the $Ru(NH_3)_6^{2+/3+}$ couple as a standard where $\pi$ bonding is not a factor in either oxidation state.

**Table VI.** Formal Reduction Potential of $Ru(py)_6^{3+/2+}$ and Related Ruthenium Complexes

| complex | $E_f$[a] | $\Delta E$, V[b] | $\Delta E \times 10^{-3}$, cm$^{-1}$ | ref |
|---|---|---|---|---|
| $Ru(NH_3)_6^{3+/2+}$ | 0.05 | 0.00 | 0.0 | 38 |
| $Ru(NH_3)_5py^{3+/2+}$ | 0.30 | 0.25 | 2.0 | 38 |
| *trans*-$Ru(NH_3)_4py_2^{3+/2+}$ | 0.49 | 0.44 | 3.5 | 38 |
| *cis*-$Ru(NH_3)_4py_2^{3+/2+}$ | 0.51 | 0.46 | 3.7 | 38 |
| $Ru(NH_3)_6^{3+/2+}$ | 0.12[c] | 0.00 | 0.0 | 42 |
| $Ru(py)_6^{3+/2+}$ | 1.29[c] | 1.17 | 9.4 | this work |

[a] In volts vs. the NHE; measured in an aqueous solution of 0.10 M *p*-toluenesulfonic acid–0.10 M potassium *p*-toluenesulfonate unless otherwise noted. [b] $\Delta E = E_f$[complex] $- E_f[Ru(NH_3)_6^{3+/2+}]$. [c] In volts vs. the SCE; measured in an acetonitrile solution of 0.10 M $[(C_4H_9)_4N][PF_6]$ as a supporting electrolyte.

Rather than attributing the variation in redox potential for various ruthenium 2+/3+ couples solely to $\pi$ stabilization energies one may invoke a rationale involving the average energy of the d$\pi$ orbitals from which the electron will be removed. Assume that the energy of the $t_{2g}$ orbitals is fixed by the dominant bonding forces inherent in octahedral metal complexes, and correlate these levels with thermodynamic energies as reflected in potential measurements. Splitting of the degenerate d$\pi$ levels due to perturbations by $\pi$ interactions can occur in a subsequent step. As a very crude method of estimating the change in $\delta$ we may correlate the change in the $t_{2g}$ energy level with the difference in the potential of the respective 2+/3+ couples based on the above arguments. The data taken from Table VI then suggest that $\delta_{2t} = \delta_{2c} - 0.2 = 22.0 \times 10^3$ cm$^{-1}$ while $\delta_1 = \delta_{2c} - 1.7 = 20.5 \times 10^3$ cm$^{-1}$ where $\delta_n$ is the $\alpha_L - \alpha_{Ru}$ term for $(NH_3)_{6-n}Ru(py)_n^{2+}$ with c and t denoting cis and trans, respectively. The corresponding $\delta$ value for $Ru(NH_3)_6^{2+}$ would then be $\delta_0 = \delta_{2c} - 3.7 = 18.5 \times 10^3$ cm$^{-1}$, but of course this only provides a hypothetical reference point since there are no pyridine $\pi^*$ orbitals present in the hexaammineruthenium complex.

Once $\delta$ has been deduced in this manner it is possible to calculate a unique value of $\beta$ for each complex based on the energy of the observed MLCT band. The results are tabulated in Table VII where $\Delta E(\pi)$ is the $\pi$ stabilization energy for each perturbed metal d$\pi$ orbital.

Although the assumptions required to obtain the semiquantitative estimates of the $\delta$ and $\beta$ molecular orbital parameters above are sufficiently crude so as to erode confidence in the exact numerical values which result, several desirable features are present in the trends which are evident.

Firstly, the variation in $\delta$ as extracted from potential measurements is consistent with all of the observed spectral features. In fact the compatibility of the electrochemical and charge-transfer data is quite gratifying as reflected in the $\beta$ values which are dependent on the choice of $\delta$ as dictated by potential measurements for each complex.

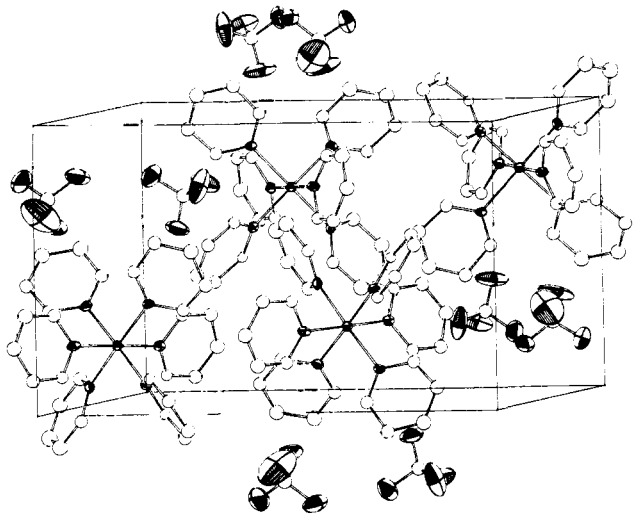

Figure 2. A view of the unit cell contents of $[Ru(py)_6][BF_4]_2$.

Secondly, the paradoxical energy of the MLCT band in the trans complex relative to the monopyridine case is accounted for by a decrease in $\beta$ even though $\delta$ increases as one would expect. In this model the orientation of the two pyridine ligands need not be coplanar while coplanarity is required in the Zwickel and Creutz analysis to assure the presence of a low-energy nonbonding ligand $\pi^*$ combination.[39] Certainly one anticipates that if $\pi$ bonding plays a role in the energetics of the metal–ligand interactions the trans pyridine ligands would attempt to maintain an almost exclusive orthogonal orientation with respect to one another in order to minimize competition for the available $d\pi$ electron density. The increased $\delta$ value and decreased $\beta$ value associated with the trans complex as compared to $[(NH_3)_5Ru(py)]^{2+}$ are consistent with a description based on a trans influence originating in the $\sigma$ bonds. This result is more intuitively appealing than schemes which require coplanarity of trans pyridine ligands with no steric justification requiring such a geometry.

Thirdly, the transition intensity as reflected by the respective extinction coefficients suggests that the single MLCT band observed in *trans*-$[(NH_3)_4Ru(py)_2]^{2+}$ consists of two degenerate transitions as contrasted with the cis case where two distinct bands are observed. If the trans complex was displaying only one allowed transition to a nonbonding $\pi^*$ ligand combination with the second transition to a higher lying antibonding ($\pi^* + t_{2g}$) orbital being forbidden one would expect the intensity to be similar to that of the lower energy band in the cis complex which is derived from exactly this type of transition; this is not the case.

Finally, it should be noted that the value of $\beta$ calculated for $Ru(py)_6^{2+}$ is near that of the trans tetraammine complex as one would anticipate. The relatively large $\delta$ value of $27.9 \times 10^3$ $cm^{-1}$ for the hexapyridineruthenium(II) cation is indicative of a substantial increase in the effective nuclear charge of the metal relative to complexes with two or less pyridine ligands.

While the relatively weak absorption at 272 nm cannot be definitively assigned, it is conceivable that this could be a d–d transition appearing as a shoulder located between the two more intense electronic absorptions. Such an assignment would nearly match the $^1A_{1g} \rightarrow {}^1T_{2g}$ transition energy of $36.4 \times 10^3$ $cm^{-1}$ reported for $Ru(NH_3)_6^{2+}$ ($\epsilon$ 624).[40] The hexaammineruthenium exhibits a second feature at lower energy (ca. 400 nm, $\epsilon \approx 30$),[40] but any analogous $^1A_{1g} \rightarrow {}^1T_{1g}$ transition in $Ru(py)_6^{2+}$ would almost certainly be buried beneath the broad MLCT band.

**Electrochemistry.** The electrochemical properties of $[Ru(py)_6][BF_4]_2$ virtually mimic those of $Ru(bpy)_3^{2+}$. The $[Ru(py)_6]^{2+}$ complex undergoes a reversible one-electron oxidation at a potential of 1.29 V (vs. SCE) in 0.10 M $[Bu_4N][PF_6]$–$CH_3CN$ as determined by cyclic voltammetry. This potential is equal to the formal reduction potential reported for the $Ru(bpy)_3^{3+/2+}$ couple in acetonitrile.[41] Cyclic voltammograms were measured at scan rates from 50 to 500 mV/s and the peak potential separation of 70 mV was considered indicative of reversible electron transfer between the $[Ru(py)_6]^{3+/2+}$ couple.

Exhaustive electrolysis of an acetonitrile solution of $[Ru(py)]_6^{2+}$ at a constant potential (1.50 V) more anodic than $E_{1/2}$ on the diffusion plateau of the voltammetric wave led to a quantitative one-electron oxidation of the complex cation ($n$ = 0.97 from coulometric measurements). The cyclic voltammogram obtained following electrolysis was identical with the initial voltammogram in accord with a reversible oxidation of $[Ru(py)_6]^{2+}$ to $[Ru(py)_6]^{3+}$.

The dramatic difference in $E_{1/2}$ values for $Ru(NH_3)_6^{3+/2+}$ (0.12 V)[42] and $Ru(py)_6^{3+/2+}$ (1.29 V) reinforces conclusions regarding the interplay between $\pi$ and $\sigma$ effects which was alluded to previously. The origin of the ligand field strength of ammonia is evident in the molecular orbital description of $Ru(NH_3)_6^{2+}$ as the difference between the $e_g^*$ antibonding orbitals and the $t_{2g}$ metal orbitals which are rigorously nonbonding. Pyridine is a weaker $\sigma$ donor than ammonia and this chemical feature manifests itself as a smaller increase in energy for the $\sigma^*$ metal orbitals of $e_g$ symmetry relative to the ammonia case. However, the empty $\pi^*$ orbitals available on pyridine introduce ligand orbitals capable of interacting with the metal $d\pi$ set of orbitals, and the $t_{2g}$ metal orbitals are no longer constrained to be nonbonding. The resultant metal–ligand $\pi$ overlap lowers the $t_{2g}$ energy level relative to the nonbonding case. Since $10Dq$ is determined by the energy difference between $e_g^*$ and $t_{2g}$, lowering the $t_{2g}$ energy level has the same effect as raising the $e_g^*$ level. In comparing ammonia and pyridine the ability to mix ligand character into the $d\pi$ orbitals is unique to pyridine. The upshot of the weaker lone pair $\sigma$ donation from pyridine combined with some back $\pi$ donation from the metal is a splitting of the $e_g^*$ and $t_{2g}$ levels which is fortuitously close to that caused by ammonia via a $\sigma$-only mechanism.

Ammonia, as a strong $\sigma$-only ligand, will prefer to bond to the higher oxidation state metal center present in ruthenium(III) complexes while pyridine, as a $\pi$ acid ligand, will avail itself of the electron density accessible in $d^6$ ruthenium(II) complexes. While $10Dq$ reflects the energy difference between metal orbitals in a specific complex as determined by $\sigma$ and $\pi$ effects, the oxidation potential is strictly a thermodynamic quantity equal to the difference in the total energy of the $RuL_6^{2+}$ and $RuL_6^{3+}$ ions in solution. The large difference in redox potentials between the ammine and pyridine complexes emphasizes the disparate bonding mechanisms at work in the two cases.

Table VII. Molecular Orbital Parameters[a] Calculated from Band Maxima and Reduction Potentials

| complex | $\delta \times 10^{-3}$, $cm^{-1}$ | $\beta \times 10^{-3}$, $cm^{-1}$ | $E(\pi) \times 10^{-3}$, $cm^{-1}$ |
|---|---|---|---|
| $Ru(NH_3)_6^{2+}$ | 18.5 | 0 | 0 |
| $Ru(NH_3)_5py^{2+}$ | 20.5 | 6.7 | 2.0 |
| *trans*-$Ru(NH_3)_4py_2^{2+}$ | 22.0 | 4.3 | 0.8 |
| *cis*-$Ru(NH_3)_4py_2^{2+}$ | 22.2 | 5.2 | 2.2 |
| $Ru(py)_6^{2+}$ | 27.9 | 4.5 | 0.7 |

[a] $\delta$ and $\beta$ are defined as in ref 39 with $\delta = \alpha_L - \alpha_{Ru}$ and $\beta = (\pi^*|H|t_{2g})$ while $E(\pi)$ is the stabilization energy per orbital calculated as the energy difference between the pure metal $t_{2g}$ level and the bonding molecular orbital consisting of ($t_{2g} + \pi^*$) character.

**Table VIII.** Molecular Geometry of $[Ru(NC_5H_5)_6][BF_4]_2$

A. Intramolecular Bond Distances (Å)

(1) Ruthenium Coordination Sphere

| | | | |
|---|---|---|---|
| Ru-N(1) | 2.10(1) | Ru-N(4) | 2.12(1) |
| Ru-N(2) | 2.11(1) | Ru-N(5) | 2.12(1) |
| Ru-N(3) | 2.14(1) | Ru-N(6) | 2.12(1) |

(2) Pyridine Ligands

| | | | |
|---|---|---|---|
| N(1)-1C(1) | 1.34(2) | N(1)-1C(5) | 1.39(2) |
| 1C(1)-1C(2) | 1.37(2) | 1C(5)-1C(4) | 1.33(2) |
| 1C(2)-1C(3) | 1.38(2) | 1C(4)-1C(3) | 1.40(2) |
| N(2)-2C(1) | 1.35(2) | N(2)-2C(5) | 1.33(2) |
| 2C(1)-2C(2) | 1.41(2) | 2C(5)-2C(4) | 1.43(2) |
| 2C(2)-2C(3) | 1.36(2) | 2C(4)-2C(3) | 1.39(2) |
| N(3)-3C(1) | 1.32(2) | N(3)-3C(5) | 1.31(2) |
| 3C(1)-3C(2) | 1.37(2) | 3C(5)-3C(4) | 1.42(2) |
| 3C(2)-3C(3) | 1.37(2) | 3C(4)-3C(3) | 1.39(2) |
| N(4)-4C(1) | 1.33(2) | N(4)-4C(5) | 1.37(2) |
| 4C(1)-4C(2) | 1.45(2) | 4C(5)-4C(4) | 1.40(2) |
| 4C(2)-4C(3) | 1.36(2) | 4C(4)-4C(3) | 1.38(2) |
| N(5)-5C(1) | 1.39(2) | N(5)-5C(5) | 1.35(2) |
| 5C(1)-5C(2) | 1.43(2) | 5C(5)-5C(4) | 1.38(2) |
| 5C(2)-5C(3) | 1.39(2) | 5C(4)-5C(3) | 1.38(2) |
| N(6)-6C(1) | 1.35(2) | N(6)-6C(5) | 1.33(2) |
| 6C(1)-6C(2) | 1.39(2) | 6C(5)-6C(4) | 1.38(2) |
| 6C(2)-6C(3) | 1.38(2) | 6C(4)-6C(3) | 1.35(2) |

(3) Tetrafluoroborate Anions

| | | | |
|---|---|---|---|
| B(1)-1F(1) | 1.35(2) | B(2)-2F(1) | 1.35(3) |
| B(1)-1F(2) | 1.21(2) | B(2)-2F(2) | 1.22(3) |
| B(1)-1F(3) | 1.38(3) | B(2)-2F(3) | 1.26(3) |
| B(1)-1F(4) | 1.25(2) | B(2)-2F(4) | 1.21(3) |

B. Intramolecular Bond Angles (deg)

(1) Ruthenium Coordination Sphere

trans N-Ru-N angles

| | | | |
|---|---|---|---|
| N(1)-Ru-N(2) | 176.7(5) | | |
| N(3)-Ru-N(4) | 176.0(4) | | |
| N(5)-Ru-N(6) | 178.4(5) | | |

cis N-Ru-N angles

| | | | |
|---|---|---|---|
| N(1)-Ru-N(3) | 87.1(4) | N(3)-Ru-N(5) | 89.4(4) |
| N(3)-Ru-N(2) | 92.5(4) | N(5)-Ru-N(4) | 86.6(4) |
| N(2)-Ru-N(4) | 87.2(4) | N(4)-Ru-N(6) | 92.0(4) |
| N(4)-Ru-N(1) | 93.4(4) | N(6)-Ru-N(3) | 92.0(4) |
| | 360.2 | | 360.0 |
| N(1)-Ru-N(5) | 92.7(5) | | |
| N(5)-Ru-N(2) | 90.6(4) | | |
| N(2)-Ru-N(6) | 88.4(4) | | |
| N(6)-Ru-N(1) | 88.3(5) | | |
| | 360.0 | | |

(2) In-Plane Ru-N-C

| | | | |
|---|---|---|---|
| Ru-N(1)-1C(1) | 125.2(9) | Ru-N(1)-1C(5) | 119.9(9) |
| Ru-N(2)-2C(1) | 118.5(10) | Ru-N(2)-2C(5) | 122.7(10) |
| Ru-N(3)-3C(1) | 119.1(9) | Ru-N(3)-3C(5) | 123.6(10) |
| Ru-N(4)-4C(1) | 118.8(11) | Ru-N(4)-4C(5) | 123.2(9) |
| Ru-N(5)-5C(1) | 119.9(9) | Ru-N(5)-5C(5) | 123.7(9) |
| Ru-N(6)-6C(1) | 121.0(9) | Ru-N(6)-6C(5) | 123.2(10) |

(3) Pyridine Ligands

| | | | |
|---|---|---|---|
| 1C(1)-N(1)-1C(5) | 114.7(11) | 1C(2)-1C(3)-1C(4) | 119.2(16) |
| N(1)-1C(1)-1C(2) | 124.3(12) | N(1)-1C(5)-1C(4) | 125.1(14) |
| 1C(1)-1C(2)-1C(3) | 118.4(14) | 1C(5)-1C(4)-1C(3) | 118.1(15) |
| 2C(1)-N(2)-2C(5) | 118.8(13) | 2C(2)-2C(3)-2C(4) | 119.1(17) |
| N(2)-2C(1)-2C(2) | 121.3(14) | N(2)-2C(5)-2C(4) | 122.5(15) |
| 2C(1)-2C(2)-2C(3) | 120.3(15) | 2C(5)-2C(4)-2C(3) | 117.8(16) |
| 3C(1)-N(3)-3C(5) | 117.2(13) | 3C(2)-3C(3)-3C(4) | 120.3(17) |
| N(3)-3C(1)-3C(2) | 124.2(14) | N(3)-3C(5)-3C(4) | 124.8(14) |
| 3C(1)-3C(2)-3C(3) | 118.1(15) | 3C(5)-3C(4)-3C(3) | 115.3(15) |
| 4C(1)-N(4)-4C(5) | 118.0(13) | 4C(2)-4C(3)-4C(4) | 121.4(19) |
| N(4)-4C(1)-4C(2) | 122.5(16) | N(4)-4C(5)-4C(4) | 122.7(14) |
| 4C(1)-4C(2)-4C(3) | 117.2(17) | 4C(5)-4C(4)-4C(3) | 118.0(17) |
| 5C(1)-N(5)-5C(5) | 116.3(12) | 5C(2)-5C(3)-5C(4) | 118.6(16) |
| N(5)-5C(1)-5C(2) | 121.2(13) | N(5)-5C(5)-5C(4) | 124.4(13) |
| 5C(1)-5C(2)-5C(3) | 119.4(14) | 5C(5)-5C(4)-5C(3) | 119.9(15) |
| 6C(1)-N(6)-6C(5) | 115.6(12) | 6C(2)-6C(3)-6C(4) | 119.6(17) |
| N(6)-6C(1)-6C(2) | 125.3(13) | N(6)-6C(5)-6C(4) | 122.9(15) |
| 6C(1)-6C(2)-6C(3) | 116.2(14) | 6C(5)-6C(4)-6C(3) | 120.3(17) |

(4) Tetrafluoroborate Anions

| | | | |
|---|---|---|---|
| 1F(1)-B(1)-1F(2) | 112(2) | 1F(2)-B(1)-1F(3) | 106(2) |
| 1F(1)-B(1)-1F(3) | 109(2) | 1F(2)-B(1)-1F(4) | 121(3) |
| 1F(1)-B(1)-1F(4) | 105(2) | 1F(3)-B(1)-1F(4) | 104(2) |
| 2F(1)-B(2)-2F(2) | 109(2) | 2F(2)-B(2)-2F(3) | 109(3) |
| 2F(1)-B(2)-2F(3) | 113(2) | 2F(2)-B(2)-2F(4) | 112(3) |
| 2F(1)-B(2)-2F(4) | 111(3) | 2F(3)-B(2)-2F(4) | 104(3) |

**Description of the Structure.** The structure consists of one discrete hexapyridineruthenium(II) cation and two fluoroborate anions per asymmetric quarter of the unit cell (see Figure 2). The structure of the complex cation is illustrated more clearly by a perspective view along one of the pseudooctahedral threefold axes in Figure 3. The interatomic distances and angles of interest are listed in Table VIII.

In contrast to the $T_h$ geometry which was anticipated for the $Ru(py)_6^{2+}$ complex based on the assumption that it would resemble the known hexapyridineiron(II) structure,[9] the orientation of the pyridine rings in the six-coordinate ruthenium(II) cation is such that no symmetry element exists for the metal complex in the solid state. Rather than adopting a coplanar orientation of trans pyridines the three pairs of trans ligands (1,2; 3,4; 5,6) deviate from coplanarity by 90.7, 65.6, and 29.9°, respectively. The electronic and/or steric factors which dictate that such a low symmetry should prevail in this complex are not readily apparent. A molecular propeller is observed as one traverses any plane containing the ruthenium and four nitrogen atoms, although the angular direction of the four blades is not always consistent (vide infra). The result is an octahedral metal complex with six equivalent ligands that is chiral in the solid state.

The six nitrogen atoms surround the metal in an octahedral

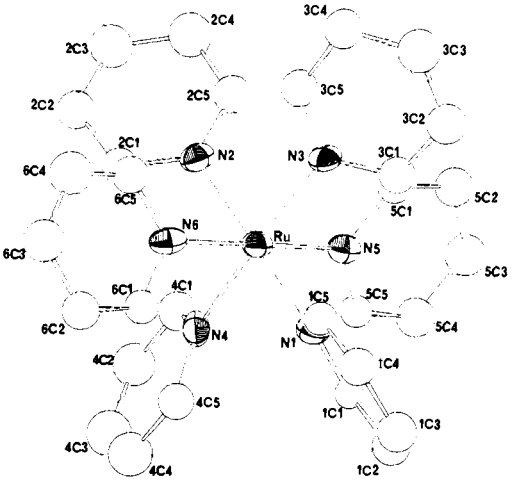


**Figure 3.** A perspective view of the $[Ru(py)_6]^{2+}$ cation down one of the pseudo-threefold octahedral axes showing the atomic labeling scheme.

fashion with 176.0° ≤ *trans*-(∠N-Ru-N) ≤ 178.4° and 86.6° ≤ *cis*-(∠N-Ru-N) ≤ 93.4°. The Ru-N distances vary from 2.10 (1) to 2.14 (1) Å. These Ru-N distances are in the range

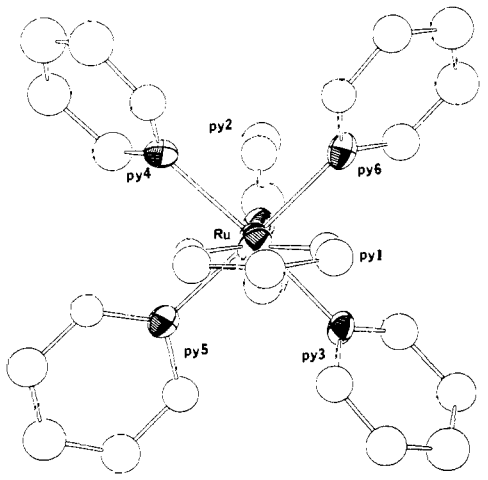


Figure 4. A perspective view of the $[Ru(py)_6]^{2+}$ cation down the py1-Ru-py2 axis.

previously reported for $Ru(NH_3)_6^{2+}$ (2.144 Å)[36] and $Ru(NH_3)_6^{3+}$ (2.104 Å)[36] and slightly elongated relative to $[(py)_4Ru(ox)Ru(py)_4]^{2+}$ (2.066–2.095 Å).[19] It should be noted that the long Fe–N distances in $Fe(py)_6^{2+}$ (2.22–2.29 Å)[9] reflect the high-spin ($t_{2g}^4e_g^2$) configuration which causes considerable bond lengthening due to two d electrons in the $\sigma^*(e_g)$ orbitals. Quantitative confirmation of the influence of a high-spin configuration on iron(II)-nitrogen bond lengths has recently been reported where a decrease of 0.19 Å was found for the average Fe(II)–N bond distance in the tris($\alpha$-picolylamine) low-spin complex relative to the analogous high-spin compound.[43]

Any attempt to rationalize the seemingly incoherent rotational orientation of the six pyridines in terms of intramolecular electronic effects should be preceded by an evaluation of other factors which could mandate such an arrangement. In particular one must carefully consider fluorine–hydrogen distances in a search for distortional forces which could alter the geometry of the complex cation. Location of the hydrogen atoms (assuming a $C(sp^2)$–H bond distance of 0.95 Å) allows one to calculate the hydrogen–fluorine atomic separations. Typical values for hydrogen–fluorine distances for hydrogen bonds to fluorine vary from 1.10 to 1.60 Å[44] while the shortest distance between any H–F pair in the $[Ru(py)_6][BF_4]_2$ structure is considerably greater than 2.0 Å (2.35 Å for the *p*-H of ring 3, a distance which is independent of rotation since the hydrogen is in the para position). There are six other H–F separations between 2.44 and 2.50 Å with all others greater than 2.5 Å. On this basis the observed solid-state structure of $Ru(py)_6^{2+}$ is assumed to result from forces within the cation itself. The absence of hydrogen bonding between fluorines and the aromatic hydrogens is not surprising.

Steric repulsion among the six pyridine ligands is centered at the ortho protons. A few moments spent with model structures confirm the conclusion of Doedens and Dahl[9] that the steric energy is minimized when $T_h$ symmetry is adopted by the hexapyridine metal moiety. Although this point group is not common, other examples of octahedral complexes with $T_h$ symmetry include $W(N(CH_3)_2)_6$[45] and $M(NO_2)_6^{n-}$[46] If intramolecular ortho hydrogen contacts were the dominant force in determining the solid-state conformation of the cation it is clear that a structure quite different than the one observed for $[Ru(py)_6][BF_4]_2$, such as the $T_h$ geometry of $Fe(py)_6^{2+}$ where the high-spin configuration and the size of the metal negate metal-to-ligand $\pi$ bonding, would have been found. One is left to ponder asymmetric intramolecular electronic interactions to account for the pyridine orientations.

It is possible to understand the rotational orientation of the pyridine ligands in the following manner, where the term "understand" is intended to imply only an ex post facto rationalization of the observed structure. The rationale itself is only slightly above the level of a mnemonic for reconstructing the solid-state conformation. One may profitably construct hexapyridineruthenium(II) by the stepwise addition of two trans ligands at a time. The first pyridine can be bound along the $z$ axis, and the orientation of the plane is arbitrary since the $\sigma$ bond is independent of rotation and the $(d_{xz}, d_{yz})$ orbitals are degenerate and describe a two-dimensional function space such that a linear combination will optimize the metal-to-ligand $\pi$ stabilization regardless of the particular rotamer involved. Addition of the trans pyridine is no longer unrestricted with respect to the orientation of the planar ligand since the $(d_{xz}, d_{yz})$ degeneracy of the free $Ru^{2+}$ ion has been destroyed. An absence of steric restraints characterizes the hypothetical *trans*-$Ru(py)_2^{2+}$ moiety, so it is clear that electronic effects will fix the geometry. The two pyridine planes would then adopt perpendicular orientations in order to avoid competing for the same $d\pi$ electron density. This perpendicular relationship of the trans pyridine planes would be expected to prevail regardless of the magnitude of the stabilization attributable to $\pi$ bonding as long as it is nonzero.

The same analysis is applicable to the next pair of trans pyridine ligands with the stipulation that steric repulsion may prohibit the hypothetical $Ru(py)_4^{2+}$ fragment from realizing certain conformations that would be electronically favorable. One would anticipate that the second pair of ligands would again eliminate competition for the same $d\pi$ orbital by maintaining a perpendicular orientation relative to one another if possible. Two pairs of trans ligands will define a square plane about the ruthenium. Two limiting possibilities exist: (1) to form the new pair of ruthenium–nitrogen bonds in the plane of one of the first pyridines; (2) to form the two additional

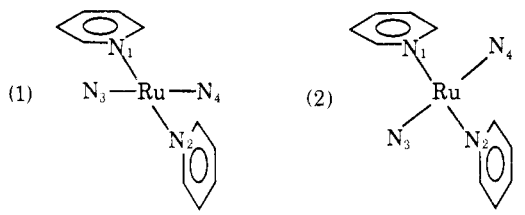


Ru–N bonds at 45° relative to both of the original pyridines. Only case (2) can accommodate a perpendicular relationship between both sets of trans ligands simultaneously. Such a conformation is prohibited in case (1) since two cis pyridines would be coplanar and the adjacent ortho protons of these two ligands would be nearly superimposed on one another. The net result of the above deductions is a four-bladed propeller with each blade inclined at 45°. In the absence of an electronic $\pi$ argument favoring this rotamer the obvious geometric choice would have been a vertical orientation of each of the four pyridine planes relative to the square-planar $RuN_4$ fragment. Such an arrangement would allow only one of the three $d\pi$ orbitals to be involved in $\pi$ bonding, however, as contrasted with the propeller model which allows all three metal $d\pi$ orbitals to have nonzero matrix elements with ligand $\pi^*$ orbitals.

Addition of the final pair of trans pyridine ligands is subject to substantially greater steric restrictions than the second set of two. The crux of the conflict is evident when one recognizes that it is impossible to maintain a simultaneous propeller configuration with a compatible helical sense for both of the resultant $Ru(py)_4$ fragments containing the final pair of pyridines. It is possible to orient ligands 5 and 6 with respect to 1 and 2 such that the $Ru(py)_4$[1,5,2,6] system will be optimal with a consistent canting angle of 45° for each pyridine and

**Table IX.** Dihedral Angles between Pyridine Rings and $RuN_4$ Equatorial Planes

| equatorial plane | pyridine label | cant angle, deg |
|---|---|---|
| Ru(py)$_4$[1,3,2,4] | 1 | +47.0 |
| | 3 | +34.8 |
| | 2 | +43.9 |
| | 4 | +31.0 |
| Ru(py)$_4$[1,5,2,6] | 1 | −44.5 |
| | 5 | +68.0 |
| | 2 | −46.8 |
| | 6 | −38.3 |
| Ru(py)$_4$[3,5,4,6] | 3 | −55.9 |
| | 5 | −24.5 |
| | 4 | −58.5 |
| | 6 | +54.5 |

both trans pairs will consist of orthogonal pyridines. The impediment to attaining this structure is that the Ru(py)$_4$[3,5,4,6] fragment will then have alternate pyridines canted at angles of +45 and −45° and four extremely unfavorable ortho interactions result. Such a configuration seems unreasonable on steric grounds.

The model developed can still be salvaged if one compromises the electronic factors which favor orthogonality for trans pyridines with steric factors. Given that the fifth pyridine will encounter significant steric repulsion one can attempt to minimize this repulsive energy term by perturbing the orientation of ligands 3 and 4. Specifically one can position the fifth pyridine with the sense of the slant reversed relative to ligands 1 and 2 with the plane more nearly aligned vertically relative to the Ru(py)$_4$[1,5,2,6] plane to reduce the unfavorable ortho interaction which is present between pyridine 5 and pyridines 1 and 2. Pyridines 3 and 4 then rotate away from the ortho positions of 5 with the rotation limited by movement toward the ortho positions of 1 and 2. At this point the Ru(py)$_5$ fragment has a compatible orientation of ligands 3, 5, and 4 with inclination angles of >45, <45, and >45°, respectively, while the incompatible slant of pyridines 1, 5, and 2 is characterized by angles of 45, <−45, and 45°. The final coordination site is filled with a pyridine canted in the same sense as 1 and 2 but opposite to 3 and 4. Unfavorable ortho interactions are decreased by rotating ligand 6 toward the vertical with respect to the Ru(py)$_4$[3,5,4,6] plane. The net result of the above rationalization is reflected in a view of the $Ru(py)_6^{2+}$ cation along the 1-2 ligand axis (Figure 4).

It is thus possible to optimize the bonding of the first pair of trans pyridines and deduce in a systematic fashion the solid-state structure of $Ru(py)_6^{2+}$. Indeed pyridines 1 and 2 exhibit the two shortest Ru-N bonds in the complex and this feature lends support to the above conceptual framework. Unfortunately the differences in Ru-N bond lengths are not sufficiently statistically meaningful to provide definitive evidence of substantial differences among the six ruthenium-pyridine bonds. Nonetheless the observed cant angles as listed in Table IX are consistent with the combination of electronic and steric factors presented.

Further support for the bonding principles espoused here is provided by the crystal structure of $\mu$-oxalato-bis(tetrapyridineruthenium(II)) fluoroborate.[19] The trans aromatic nitrogen rings are nearly perpendicular to one another (81°) and seem to dictate the orientation of the remaining pyridine rings in spite of the longer Ru-N bond distances observed for the trans pair. The $\sigma$ bond strength will largely determine the metal-ligand bond length, but since $\sigma$ bonding is independent of ligand rotation $\pi$ effects will be the electronic component which couples with steric repulsion to establish the rotational conformation of lowest energy. In $[Ru(py)_4(ox)Ru(py)_4]^{2+}$ the cis pyridines which are trans to oxalate form angles of 46 and −56° with the $RuN_2O_2$ plane in order for each to conform to the helicity established by the trans pyridine pair. The concomitant unfavorable ortho congestion seems to be dictated by the perpendicular orientation of the trans pair of pyridine ligands.

**Acknowledgment.** This work was supported by the University Research Council of the University of North Carolina. The author wishes to thank Professor G. Wilkinson for his encouragement during the initial phases of this work at Imperial College and Professor D. J. Hodgson for generously providing crystallographic expertise as needed. The author is also indebted to Dr. P. B. Sullivan for performing the electrochemical measurements.

**Supplementary Material Available:** A listing of observed and calculated structure amplitudes (12 pages). Ordering information is given on any current masthead page.

## References and Notes

(1) H. Taube, *Surv. Prog. Chem.*, **6**, 1 (1973).
(2) F. M. Lever and A. R. Powell, *J. Chem. Soc. A*, 1477 (1969).
(3) J. Chatt, G. J. Leigh, and N. Thankarajan, *J. Chem. Soc. A*, 3168 (1971).
(4) A. D. Allen and F. Bottomley, *Acc. Chem. Res.*, **1**, 360 (1968).
(5) C. P. Anderson, D. J. Salmon, T. J. Meyer, and R. C. Young, *J. Am. Chem. Soc.*, **99**, 1980 (1977).
(6) G. Sprintschnik, H. W. Sprintschnik, P. P. Kirsch, and D. G. Whitten, *J. Am. Chem. Soc.*, **99**, 4947 (1977).
(7) G. A. Crosby, *Acc. Chem. Res.*, **8**, 231 (1975).
(8) (a) B. N. Figgis, R. D. Gillard, R. S. Nyholm, and G. Wilkinson, *J. Chem. Soc.*, 5189 (1964); (b) D. G. Holah and J. P. Fackler, Jr., *Inorg. Chem.*, **4**, 1112 (1965); (c) D. W. Herlocker and M. R. Rosenthal, *Inorg. Chim. Acta*, **4**, 501 (1970).
(9) R. J. Doedens and L. F. Dahl, *J. Am. Chem. Soc.*, **88**, 4847 (1966).
(10) B. N. Figgis, "Introduction to Ligand Fields", Interscience, New York, 1966, p 243.
(11) R. J. Young and G. Wilkinson, *J. Chem. Soc., Dalton Trans.*, 719 (1976).
(12) P. S. Hallman, T. A. Stephenson, and G. Wilkinson, *Inorg. Synth.*, **12**, 238 (1970).
(13) R. W. Mitchell, A. Spencer, and G. Wilkinson, *J. Chem. Soc., Dalton Trans.*, 846 (1973).
(14) W. J. Geary, *Coord. Chem. Rev.*, **7**, 81 (1971).
(15) P. W. R. Corfield, R. J. Doedens, and J. A. Ibers, *Inorg. Chem.*, **6**, 197 (1967).
(16) W. R. Busing and H. A. Levy, *J. Chem. Phys.*, **26**, 563 (1967).
(17) S. A. Goldfield and K. N. Raymond, *Inorg. Chem.*, **10**, 2604 (1971).
(18) J. A. Ibers and W. C. Hamilton, Ed., "International Tables for X-ray Crystallography", Vol. IV, Kynoch Press, Birmingham, England, 1974: (a) Table 2.2A; (b) Table 2.3.1.
(19) P. T. Cheng, B. R. Loescher, and S. C. Nyburg, *Inorg. Chem.*, **10**, 1275 (1971).
(20) R. D. Feltham and R. G. Hayter, *J. Chem. Soc.*, 4587 (1964).
(21) D. K. Lavallee, M. D. Baughman, and M. P. Phillips, *J. Am. Chem. Soc.*, **99**, 718 (1977).
(22) D. W. Raichart and H. Taube, *Inorg. Chem.*, **11**, 999 (1972).
(23) M. A. M. Meester, D. J. Stufkens, and K. Vrieze, *Inorg. Chim. Acta*, **15**, 137 (1975).
(24) D. K. Lavallee and E. B. Fleischer, *J. Am. Chem. Soc.*, **94**, 2583 (1972).
(25) I. C. Smith and W. G. Schneider, *Can. J. Chem.*, **39**, 1158 (1961).
(26) G. C. Levy and G. L. Nelson, "Carbon-13 Nuclear Magnetic Resonance for Organic Chemists", Wiley-Interscience, New York, 1972, p 140.
(27) C. H. Kline and J. Turkevich, *J. Chem. Phys.*, **12**, 300 (1944).
(28) N. S. Gill, R. H. Nuttall, D. W. Scaife, and D. W. A. Sharp, *J. Inorg. Nucl. Chem.*, **18**, 79 (1961).
(29) R. J. H. Clark and C. S. Williams, *Inorg. Chem.*, **4**, 350 (1965).
(30) N. N. Greenwood, *J. Chem. Soc.*, 3811 (1959).
(31) K. Nakamoto, "Infrared Spectra of Inorganic and Coordination Compounds", 2nd ed., Wiley-Interscience, New York, 1970, pp 152-156.
(32) H. H. Claassen, *J. Chem. Phys.*, **30**, 968 (1959).
(33) W. P. Griffith, *J. Chem. Soc., A*, 899 (1966).
(34) M. B. Fairey and R. J. Irving, *Spectrochim. Acta*, **22**, 359 (1966).
(35) A. D. Allen and C. V. Senoff, *Can. J. Chem.*, **45**, 1337 (1967).
(36) H. C. Stynes and J. A. Ibers, *Inorg. Chem.*, **10**, 2304 (1971).
(37) P. Ford, De F. P. Rudd, R. Gaunder, and H. Taube, *J. Am. Chem. Soc.*, **90**, 1187 (1968).
(38) T. Matsubara and P. C. Ford, *Inorg. Chem.*, **15**, 1107 (1976).
(39) A. M. Zwickel and C. Creutz, *Inorg. Chem.*, **10**, 2395 (1971).
(40) H. H. Schmidtke and D. Garthoff, *Helv. Chim. Acta*, **49**, 2039 (1966).
(41) C. T. Lin, W. Bottcher, M. Chou, and N. Sutin, *J. Am. Chem. Soc.*, **98**, 6536 (1976).
(42) P. B. Sullivan, private communication.
(43) A. M. Greenaway and E. Sinn, *J. Am. Chem. Soc.*, **100**, 8080 (1978).
(44) L. Pauling, "The Nature of the Chemical Bond", Cornell University Press, Ithaca, N.Y., 1960, pp 460-464.
(45) D. C. Bradley, M. H. Chisholm, and M. W. Extine, *Inorg. Chem.*, **16**, 1791 (1977).
(46) H. Elliott, B. J. Hathaway, and R. C. Slade, *Inorg. Chem.*, **5**, 669 (1966).